Convenient method for calibrating system constant of scanning water vapor Raman lidar

Peitao Zhao (赵培涛)[1*], Yinchao Zhang (张寅超)[3], Wei Li (李 伟)[1], Shunxing Hu (胡顺星)[2], Kaifa Cao (曹开法)[2], Shaolin Wang (汪少林)[2], and Huanling Hu (胡欢陵)[2]

[1] *Meteorological Observation Centre, China Meteorological Administration, Beijing 100081, China*

[2] *Anhui Institute of Optics and Fine Mechanics, Chinese Academy of Sciences, Hefei 230031, China*

[3] *Department of Optical Engineering, Beijing Institute of Technology, Beijing 100081, China*

[*] *E-mail: peitaozhao@163.com*

Received October 27, 2009

Lower tropospheric water vapor measurements are performed at nighttime using the mobile atmosphere monitoring lidar-2 (AML-2) which is operated by the Anhui Institute of Optics and Fine Mechanics. In this lidar system, a 354.7-nm light from a Nd:YAG laser is used as stimulating source, whose Raman shifted center wavelengths are at 386.7 and 407.5 nm for nitrogen and water vapor, respectively. We present a novel and convenient method for determining the Raman lidar calibration constant according to the scanning performance of this lidar. We are likewise able to realize the measurement of water vapor profile in the low troposphere. The error induced by the uncertainty of calibrated constants is within 7% for the Raman lidar system. Experimental results from two months of study indicate that the method of calibrating the lidar system constant is feasible, and the Raman lidar performance is stable and reliable.

OCIS codes: 010.1290, 010.3640, 280.1310, 280.3640.

doi: 10.3788/COL20100806.0541.

Water vapor in the troposphere plays an important role in atmospheric radiations, climate changes, and cloud formation. Thus, continuous water vapor monitoring is very important for understanding and modeling such processes[1]. The Raman lidar system is a reliable tool for water vapor measurement[2,3]. A Raman lidar system developed by Sherlock *et al*. shows strong detecting capabilities for measuring middle and upper tropospheric water vapors; meanwhile, other systems with different functions have been developed and applied in science experiments and meteorological observations as well[4−6].

This letter presents a scanning Raman lidar system capable of measuring water vapor mixing ratio profile with sufficient reliability to allow continuous nighttime operation. This Raman lidar system can collect and retrieve near ground data signals effectively. Emphasis is given to the introduction of a calibration method for the proposed Raman lidar system. With the benefits of scanning performance, we can obtain the horizontal signals that can, in turn, be used to retrieve the water vapor mixing ratio profiles near ground. The atmosphere monitoring lidar-2 (AML-2) scanning Raman lidar equipment is also described. Results obtained from two months' worth of experiments indicate the reliability of the lidar system and the feasibility of the calibration method.

The AML-2 Raman lidar was operated at nighttime with the third harmonic frequency of a Nd:YAG laser as a light source (20-Hz repetition frequency), and pulse energy of 50 mJ at the wavelength of 354.7 nm. The collected optical telescope receiver, with a diameter of 300 mm and a tunable field of view of 0.3−2 mrad was designed as quasi-Newton mode. The vapor filter was produced by Barr Co. and devised to be insensitive to temperature. The parameters of the two Raman filters are listed in Table 1[3], where we use the full-width at half-maximum (FWHM) to represent the bandwith.

Generally, the Raman N_2 and H_2O signals are detected by a photomultiplier tube (PMT) operating in the photon-counting mode. The geometrical form factor influence of the two Raman channels for the Raman N_2 and H_2O signals can be corrected by the channel factor of this lidar. All reflective surfaces of the telescope and mirrors were coated with aluminum or medium thin film to maximize the reflection in the 200−600 nm wavelength range. With regard the operating conditions of acquisition subsystem, the parameter of pulse accumulation time was set at 10000 shots counting (about 8 min integration), while the range resolution distance was set at 30 m. The telescope was devised as a coaxial system, with a three-dimensional scanning mirror realizing the arbitrary azimuth scanning in the upper hemisphere. Figure 1 shows the detailed disposition of this lidar system.

Raman scattering is a weak molecular-scattering process characterized by a shift in scattered beam wavelength relative to the incident one. The Raman shift toward a longer wavelength is more likely to occur at typical atmospheric temperatures; this is known as the Stokes component of Raman scattering. The water vapor Raman lidar system is developed on the base of the Stokes Raman scattering principle. The vibrational wave number of N_2 corresponding to the Raman vibrational transition is 2330.7 cm^{-1}. When excited at a wavelength of 354.7 nm from a tripled Nd:YAG laser, the center of the shifted spectrum is at 386.7 nm. The Raman vibrational spectrum of water vapor shifts by approximately 3652 cm^{-1} from the exciting line. In response to the 354.7-nm radiation, the center of the water vapor Raman spectrum

Table 1. Interference Filter Characteristics and Components

Raman Filter	N_2	H_2O
Center Wavelength (nm)	386.8±0.1	407.8
FWHM (nm)	2	4.7
Peak Transmission (%)	60	55
Rejection Ration	355, 532 nm	355, 532 nm
	OD>12	OD>12
	375, 580 nm	386.7, 607 nm
	OD>7	OD>7

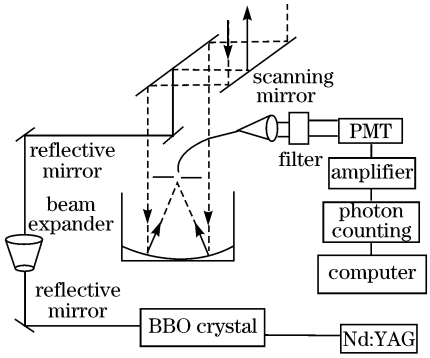

Fig. 1. Scheme scanning of the Raman lidar system.

is thus found at 407.5 nm. The collected backscattered signals of the Raman nitrogen molecular and water vapor are given by

$$S_{N_2}(z) = \frac{k_{N_2}}{z^2}\sigma_{N_2}(\pi)n_{N_2}(z)q(\lambda_0, z_0, z)q(\lambda_{N_2}, z_0, z), \quad (1)$$

$$S_{H_2O}(z) = \frac{k_{H_2O}}{z^2}\sigma_{H_2O}(\pi)n_{H_2O}(z) q(\lambda_0, z_0, z)q(\lambda_{H_2O}, z_0, z), \quad (2)$$

where $S_{N_2}(z)$ and $S_{H_2O}(z)$ are the return signals collected by nitrogen and water vapor Raman channels, respectively; $\sigma_{N_2}(\pi)$ and $\sigma_{H_2O}(\pi)$ are the backscatter cross sections for nitrogen and water vapor species caused by Raman scattering, respectively; $n_{N_2}(z)$ $n_{H_2O}(z)$ are the number densities for nitrogen and water vapor species as a function of height z, respectively; λ_0 is the wavelength of the excited beam; λ_{N_2} and λ_{H_2O} are the center wavelength of N_2 and water vapor Raman scattering, respectively. Meanwhile, $q(\lambda_{N_2}, z_0, z)$ is the transmission from the height z_0 to z at wavelength λ_{N_2} for outgoing laser beam, which is equal to $q = \exp[-\int_{z_0}^{z}\alpha_{\lambda_{N_2}}(z')\mathrm{d}z']$, where $\alpha_{\lambda_{N_2}}(z')$ is the extinction coefficient of atmosphere at the wavelength λ_{N_2}. Finally, $q(\lambda_{H_2O}, z_0, z)$ is the atmospheric transmission of backscattering signals from the height z_0 to z at wavelength λ_{H_2O}.

The water vapor mixing ratio is defined as the mass of water vapor divided by the mass of dry air in a given volume. The water vapor mixing ratio as a function of height can be expressed as[3]

$$w(z) = \frac{n_{H_2O}(z)M_{H_2O}}{n_{dry}(z)M_{dry}}, \quad (3)$$

where M_{H_2O} and M_{dry} refer to the respective molecular weights of water and dry air. Nitrogen molecule is often used as reference gas in the Raman lidar system due to its constant proportion to dry air at the heights over which these measurements are made. Thus, the Raman nitrogen return signal was used in this study to measure the mass of dry air. The water mixing ratio can be determined from lidar data by using Raman signals from water vapor and nitrogen. Using Eqs. (1) and (2), we can express the mixing ratio profiles as

$$w(z) = C_w\Delta q_w(z_0, z)\frac{S_{H_2O}(z)}{S_{N_2}(z)},$$
$$C_w = \frac{k_{N_2}}{k_{H_2O}}\frac{\sigma_{N_2}(\pi)}{\sigma_{H_2O}(\pi)}\frac{M_{H_2O}}{M_{dry}}\frac{n_{N_2}}{n_{dry}},$$
$$\Delta q_w(z_0, z) = \frac{q(\lambda_{N_2}, z_0, z)}{q(\lambda_{H_2O}, z_0, z)}, \quad (4)$$

where C_w is the system calibration constant, and $\Delta q_w(z_0, z)$ is the transmission correction function for atmospheric water vapor mixing ratio. The amount of transmission term is determined by simulation under different weather conditions. The correction value can reach 2% under the aerosol optical thickness τ =1, corresponding to quite hazy conditions between 0 and 2 km[3,7]. For practical purposes, the differential transmission influence can be neglected because the Raman lidar detecting range is within 2 km due to the original AML-2 lidar instruments disposition[8].

Determining the value of the calibration constant for this Raman lidar, which is conducted by comparing the data obtained from simultaneous radiosonde measurements, requires significant work. However, this method has shortcomings particularly in searching for ways to conduct long term absolute measurement calibration of Raman lidar systems and additional correction for the vapor mixing profiles[5,9]. Turner *et al.* calibrated the 24-h water vapor Raman lidar by comparing data with microwave radiometers (MWRs) and radiosonde during 1996 and 1997 Atmosphere Radiation Measurement (ARM) Program water vapor Intensive Observation Periods (IOP) . The calibration method used by Turner contained the correction of dead time for water vapor and nitrogen Raman channels, correction of channel overlap, and atmosphere transmission correction brought about by different atmospheric extinction conditions, and so on[10]. He also described the details of calibrated progress under "normal" and "bright" mode for the Raman lidar, and conducted comparative studies between lidar data and the chilled mirror profiles flown on the tethersonde and kite system. With the above-mentioned calibrated methods, this Raman lidar has been shown to have excellent daytime water vapor measurements without sacrificing its nighttime abilities, resulting in high-resolution measurements produced by the Raman lidar. Comparisons of lidar data with MWRs for both IOPs showed that the nighttime differences in total precipitable water vapor are within 3%, with a slight increase in daytime due to the sun radiation[10]. Another independent calibration method for the water vapor Raman lidar has been formed. Its complexity, however, proves inconvenient in applications[11]. Recently, Leblanc *et al.* described the limitations of the calibration method with radiosonde

data. Balloon-borne (radiosonde) measurement is limited by the nonsimultaneity and noncollocation of the lidar in *in situ* measurement. They proposed a hybrid calibration method using a combination of absolute calibration from radiosonde comparisons and routine-basis partial calibration using a lamp, which is characterized by the known spectra of Raman scattering. The analysis of the calibrated method suggests that accuracy rates of over 5%−10% for any application, and the suitability of the method for long-term applications can be regarded as the standard integrated approach for all water vapor lidars[12].

According to the scanning performance of AML-2 lidar, we present a new method for water vapor Raman lidar calibration. Now we provide the detailed explanation of the calibration process of the scanning Raman lidar.

Step 1: We operated the Raman lidar in horizontal and determined the quasi-calibration constant in the horizontal direction, which we processed by comparing the ratio of water vapor Raman signals to N_2 Raman signals ($\frac{S_{H_2O}(z)}{S_{N_2}(z)}$) with the data from the LI7500 H_2O analyzer. In order to improve the precision of calibration, we chose the LI7500 H_2O analyzer as standard equipment with 0.1% accuracy and set it along the lidar beam path. We then selected the average of ratios within the range of 300 m ($\frac{S_{H_2O}(0.03-0.3)}{S_{N_2}(0.03-0.3)}$) to compare with the data from LI7500 and determined the quasi-calibration constant C_1.

Step 2: We operated the Raman lidar in the vertical direction and determined the quasi-calibration constant in the same manner as that described in step 1, except that the average of ratios within the range of 60 m ($\frac{S_{H_2O}(0.03-0.06)}{S_{N_2}(0.03-0.06)}$) (the quasi-calibration constant named as C_2).

Step 3: We repeated the former steps and obtained four quasi-calibration constants and named them as C_3 and C_4. The correlation of four quasi-calibration constants was analyzed. According to some principles, such as average and least square calculation, we determined the final calibration constant of the Raman lidar from C_1, C_2, C_3 and C_4, and named it as C_w. This process is based on the assumption that the atmosphere is homogenous in horizontal within the short detecting range.

The curves in Fig. 2 represent water vapor profiles (uncalibrated) under different directions. Considering the turbulence of the atmosphere, the curves were processed by median filtering method. Figure 2(a) shows the uniform trait corresponding to the assumption of the homogeneity in the horizontal direction within the detecting range. Figure 2(b) shows two water vapor mixing ratio profiles, indicating the relative distribution of water vapor in the vertical direction.

Through a comparison with simultaneous data recorded by the LI7500 analyzer, we determined the quasi-calibration constants for the A, B, C, and D profiles in Fig. 2. The four quasi-calibration constants are denoted by C_1, C_2, C_3 and C_4, respectively. With the abovementioned calibration method, we determined the values of the quasi-calibration constants as 98 (C_1), 108 (C_2), 101 (C_3), and 102 (C_4). After analyzing the correlation between the ratio of the two Raman signals ($\frac{S_{H_2O}(z)}{S_{N_2}(z)}$) and data from the LI7500 analyzer four times, the correlation value was obtained at 0.94, and the correlation value of the four quasi-calibration constants to the ratio of two Raman signals was 0.914. The mean value of four quasi-calibration constants was 102.25, while the standard deviation was obtained at 4.19. The high correlation and small standard deviation value indicate the feasibility of the calibration method and applicability in Raman lidar calibration. The mean value was chosen as the final calibration constant, that means C_w=102.25. The details of the values of calibration process are shown in Table 2.

The values of the calibration constant determined in other days for this lidar were 108 (Aug. 26, 2007), 113 (Sep. 12, 2007), and 97 (Sep. 22, 2007). The typical measurement results are presented here. A high correlation trait was found among quasi-calibration constants, indicating that the method is reliable and that the Raman lidar system is stable. The value of calibration constant was set at 105 after several tests during two months of experimentation. After determining the calibration work for the Raman lidar and the system, the Raman lidar can be applied to the water vapor measurements conveniently. In turn, this could obtain the water mixing ratio profile by multiplying the system constant C_w to the ratio of two Raman signals ($\frac{S_{H_2O}(z)}{S_{N_2}(z)}$) directly.

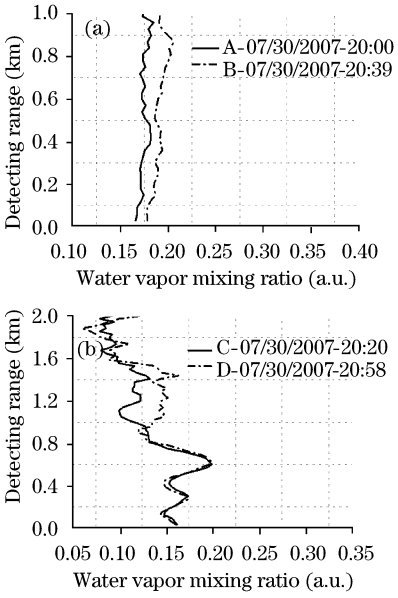

Fig. 2. Uncalibrated water vapor mixing ratio profiles in (a) horizontal and (b) vertical directions.

Table 2. Value of $S_{H_2O}(z)/S_{N_2}(z)$, Data from the LI7500 H_2O Analyzer and Quasi-Calibration Constant in Horizontal and Vertical Directions (Jul. 30, 2007)

Time	Scanning Direction	Ratio	LI7500 Data (g/m^3)	Quasi Constant
08:00	Horizontal	0.16695	16.3620	98
08:20	Vertical	0.17794	19.3780	108
08:39	Horizontal	0.16215	16.3620	101
08:58	Vertical	0.16065	16.3600	102

Figure 3 shows the mean and deviation values of the lower atmospheric water vapor mixing ratio profiles measured by the Raman lidar in the vertical direction. It should be noted that the curves include the atmosphere temporal evolution. Good agreement trait is found below 0.9-km altitude which indicates the calm atmosphere condition at that time (30-min interval). On the other hand, the stability of the Raman lidar is also proven.

During the calibration process for the water vapor Raman lidar, we applied the lidar to the Hefei area water vapor measurements several times. The detailed experiments results are presented in the following.

Figure 4 exhibits the water vapor mixing ratio profiles in the vertical direction as measured by the Raman lidar on Aug. 26, 2007. A notable distinction was found in the range from 0.9 to 1.4 km between the two profiles. This could be explained by the existence of water vapor corps at the specific altitude and dispersed under the atmospheric conditions gradually. The value of calibration constant determined by the above method was 108 for the water vapor Raman lidar system, near the value of 102.25 obtained on July 30, 2007.

Figure 5(a) exhibits the water vapor mixing ratio profiles in the horizontal direction measured by the water vapor Raman lidar on Sep. 12, 2007. Figure 5(b) exhibits the water vapor mixing ratio profiles in the vertical direction. Applying the proposed calibration method, we obtained the Raman lidar constant value at 113. In Fig. 5, water vapor mixing ratio profiles measured in the horizontal direction show equal distribution. However, the water vapor mixing ratio profiles in the vertical direction show decreasing distribution versus increasing altitude. The two water vapor mixing ratio profiles

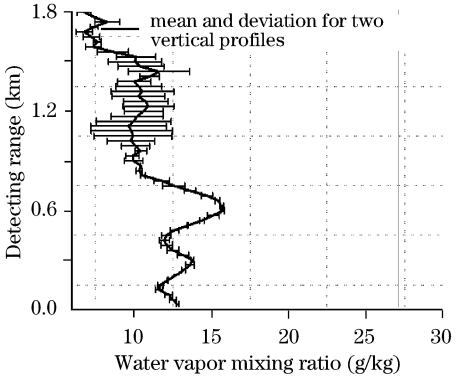

Fig. 3. Water vapor mixing ratio profile measured on Jul. 30, 2007.

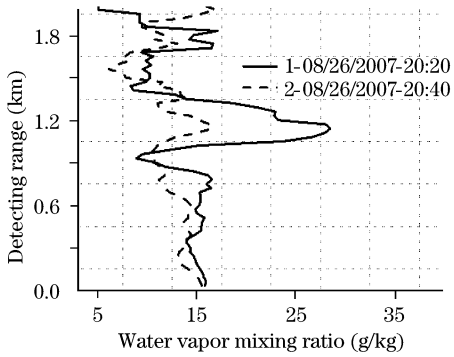

Fig. 4. Two water vapor mixing ratio profiles in the vertical direction measured on Aug. 26, 2007.

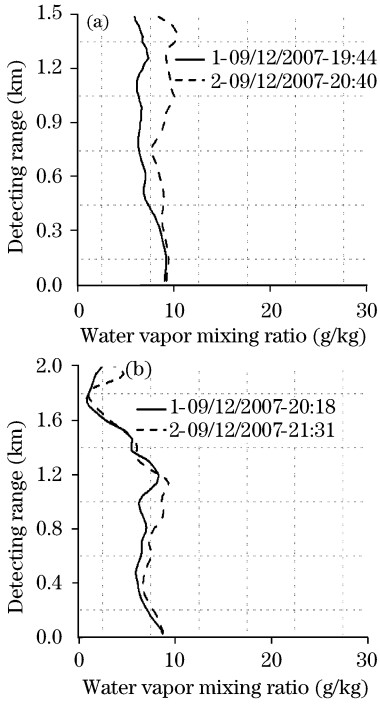

Fig. 5. Water vapor mixing ratio profiles in (a) horizontal and (b) vertical directions measured on Sep. 12, 2007.

measured by the Raman lidar are not identical, indicating that the atmosphere condition changed versus temporal evolvement. The same trait of water vapor mixing ratio profiles distribution was found in the vertical profiles. The change of water vapor mixing ratio profiles in the vertical direction in Fig. 5 is smaller than the change of profiles in Fig. 4. This can be attributed to the difference in the atmospheric conditions in these two measurements, where the conditions recorded on Aug. 26, 2007 were more active than those recorded on Sep. 12, 2007.

Figure 6 exhibits the water vapor mixing ratio profiles in the vertical direction measured on Sep. 22, 2007. The value of the Raman lidar calibration constant is 97. The distribution of water vapor mixing ratio profiles in the vertical direction measured on Sep. 22, 2007 was similar to the values measured on Sep. 12, 2007. It can be concluded that the distribution trait within the ten-day interval was stable due to the shorter time period. Figure 7 indicates the systematic error induced by the noise signals mixing with the desired water vapor Raman signals such as elastic scattering, O_2 Raman signals, etc. The deviation is smaller than 2, below the altitude of 2 km, and the influence of the noise signals can be discarded considering the perfect performance of the filter, which is used to realize the desired Raman signals extracting and noise signals rejecting. In general, the water vapor Raman lidar can be applied to monitor the water vapor mixing ratio profile, and the measurement results are in agreement with the water vapor distribution traits. At the same time, the Raman lidar system constant indicated strong stability during the two months of experimentation.

As mentioned, water vapor Raman lidar continually operated at Hefei for two months; during which four quasi-calibration constants for the Raman lidar were obtained through a comparison with data from the LI7500 H_2O

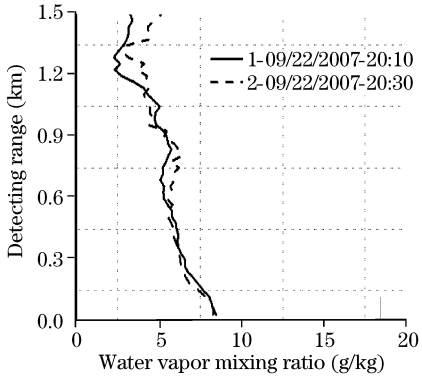

Fig. 6. Water vapor mixing ratio profiles in vertical direction measured by Raman lidar on Sep. 22, 2007.

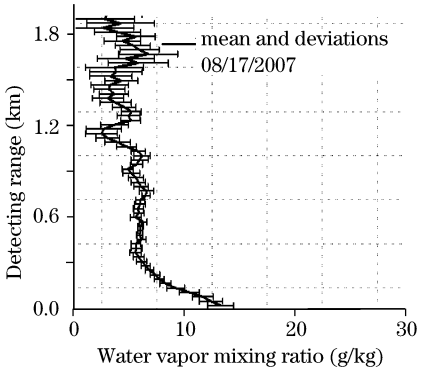

Fig. 7. Mean and deviation induced by noise signals in vertical direction measured by Raman lidar on Aug. 17, 2007.

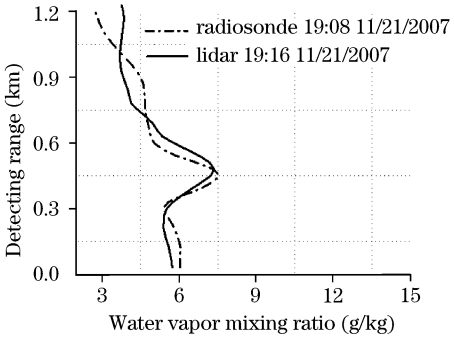

Fig. 8. Water vapor mixing ratio profiles obtained by lidar and radiosonde measurements.

analyzer. The uncertainty of calibration constant for the water vapor Raman lidar can be determined by

$$(\delta C_{\rm w})^2 = \frac{1}{N-1}\sum_{i=1}^{N}(C_{{\rm w}i} - \bar{C}_{\rm w})^2, \qquad (5)$$

where N is the total number of calibrations for the Raman lidar in different operating directions, $C_{{\rm w}i}$ is the quasi-calibration constant for each measurement, and $\bar{C}_{\rm w}$ is the average value of several quasi-calibration constants. According to the experimental results of the water vapor Raman lidar system, the error induced by uncertainty of calibration constants was small and could be within 7%.

With the calibration work for the Raman lidar finished, we conducted a comparable experiment for the water vapor Raman lidar and radiosonde on Nov. 21, 2007. Figure 8 shows the comparison results between Raman lidar and radiosonde measurements. Good agreement trait of water vapor mixing ratio could be found in two profiles. The comparison results indicate the reliability of the proposed method for calibrating system constant for the scanning Raman lidar. As shown in Fig. 8, the difference between two profiles increases with the detecting range above 1.2 km because the signal-to-noise ratio (SNR) of Raman lidar decreases in relation to the increase of detecting range. The comparison results indicate the reliability and feasibility of the calibration method, making the water vapor Raman lidar a powerful tool for monitoring the atmospheric water mixing ratio profile in atmosphere detecting field.

In conclusion, we have presented a new and convenient method for determining the calibration constant for scanning Raman lidar monitoring water vapor mixing ratio profile. Generally, the detecting range has been found to be within 2 km due to the limitations of the lidar system instruments. On the other hand, it has been found that the Raman lidar is advantageous because it could obtain the water vapor profiles near ground data reliably. Experimental results for two months' worth of continuous experiments indicate that the method is feasible, and the Raman lidar performance is stable and reliable. Furthermore, the method can be applied to other Raman lidars, such as monitoring low atmosphere CO_2 mixing ratio profile Raman lidar. This particular project is in progress.

The authors would like to thank Professor Jun Zhou and Xiaoqing Wu for their contributions to the development of this work. In addition, we wish to thank Mr. Chengsheng Ma for providing radiosonde launch support. This research was supported by the National Natural Science Foundation of China (No. 40905016) and the Science and Technology Special Basic Research of the Ministry of Science and Technology, P. R. China (No. 2007FY110700).

References

1. E. K. Schneider, B. P. Kirtman, and R. S. Lindzen, J. Atmos. Sci. **56,** 1649 (1999).
2. D. N. Whiteman, Appl. Opt. **42,** 2593 (2003).
3. D. N. Whiteman, S. H. Melfi, and R. A. Ferrare, Appl. Opt. **31,** 3068 (1992).
4. V. Sherlock, A. Garnier, A. Hauchecorne, and P. Keckhut, Appl. Opt. **38,** 5838 (1999).
5. P. Zhao, Y. Zhang, L. Wang, K. Cao, J. Su, S. Hu, and H. Hu, Chin. Opt. Lett. **6,** 157 (2008).
6. S. Wang, J. Xie, K. Cao, J. Su, P. Zhao, S. Hu, H. Wei, and H. Hu, Chinese J. Lasers (in Chinese) **35,** 739 (2008).
7. P.-T. Zhao, Y.-C. Zhang, L. Wang, Y.-F. Zhao, J. Su, X. Fang, K.-F. Cao, J. Xie, and X.-Y. Du, Chin. Phy. **16,** 2486 (2007).
8. G. Zhang, Y. Zhang, S. Hu, X. Liu, L. Yang, Z. Tao, Y. Lu, K. Cao, K. Tan, S. Shao, and H. Hu, Acta Opt. Sin. (in Chinese) **24,** 1015 (2004).
9. I. Mattis, A. Ansmann, D. Althausen, U. Wandinger, D. Mller, Y. F. Arshinov, S. M. Bobrovnikov, and I. B. Serikov, Appl. Opt. **41,** 6451 (2002).
10. D. D. Turner, J. Atmos. Ocean. Technol. **16,** 1062 (1999).
11. V. Sherlock, A. Hauchecorne, and J. Lenoble, Appl. Opt. **38,** 5816 (1999).
12. T. Leblanc and I. S. McDermid, Appl. Opt. **47,** 5592 (2008).